Vibrational spectra, tautomerism and thermodynamics of anticarcinogenic drug: 5-Fluorouracil

ARTICLE *in* SPECTROCHIMICA ACTA PART A MOLECULAR AND BIOMOLECULAR SPECTROSCOPY · MAY 2011

Impact Factor: 2.35 · DOI: 10.1016/j.saa.2011.04.008 · Source: PubMed

2 AUTHORS:

Vijay Rastogi
Easton Hospital Easton PA 18045
96 PUBLICATIONS **986** CITATIONS
SEE PROFILE

Mauricio Alcolea Palafox
Complutense University of Madrid
129 PUBLICATIONS **1,440** CITATIONS
SEE PROFILE

Spectrochimica Acta Part A 79 (2011) 970–977

Contents lists available at ScienceDirect

Spectrochimica Acta Part A: Molecular and Biomolecular Spectroscopy

journal homepage: www.elsevier.com/locate/saa

Vibrational spectra, tautomerism and thermodynamics of anticarcinogenic drug: 5-Fluorouracil

V.K. Rastogi [a,*], M. Alcolea Palafox [b]

[a] Department of Physics, CCS University, Meerut 250 004, India
[b] Departamento de Química-Física I Facultad de Ciencias Químicas, Universidad Complutense, Madrid 28040, Spain

ARTICLE INFO

Article history:
Received 2 November 2010
Received in revised form 8 March 2011
Accepted 7 April 2011

Keywords:
FT-IR, 5-Fluorouracil, B3LYP, DFT, Spectroscopy, Dimer form

ABSTRACT

The FT-IR and FT-Raman spectra of 5-Fluorouracil were recorded in the solid phase in the regions 400–4000 cm^{-1} and 50–4000 cm^{-1}, respectively. The vibrational spectra were analysed and the observed fundamentals were assigned to different normal modes of vibration. The experimental wavenumbers were compared with the scaled vibrational values using DFT methods: the Ar matrix data were related to gas phase calculations, while the values of the solid state spectra were compared to those with dimer simulations. The study indicates that some features that are characteristic of vibrational spectra of uracil and its derivatives are retained in the spectrum of 5-fluorouracil and it exists in ketonic form in the solid phase. The tautomerism was also studied and the spectra of the two most stable forms were simulated. The calculated wavenumbers have been employed to yield thermodynamic properties.

1. Introduction

It is well known that the vibrational spectra constitute an important characteristic of a molecule, and the common application of theoretical data and experimental results allow to draw detailed conclusions concerning the relation between the structure of a molecule and the exhibition of its specific properties in real conditions. The vibrational spectra also give important information for the effective investigation of H-bond formation [1].

Uracil and its derivatives, constituents of genetic materials play a pivotal role in basic biological processes. Their vibrational spectra have been studied extensively [2–13] by semiempirical [4,14] and ab initio [4,8–10,13] methods. Halogenated pyrimidines were synthesized in the 1957–1959s as potential anti-tumor agents after the successful discovery that certain tumors preferentially incorporated uracil rather than thymine into the DNA [15]. Transformation of uracil into 5-X uracil (X = halogen) significantly changes its chemical and spectroscopic properties, as well as its *in vivo* activity. They have been found to exert profound effects in a variety of microbial and mammalian agents and are used as antitumor, antibacterial and antiviral drugs. However, the mechanism of their biological activity is not fully understood and requires further studies.

5-Fluorouracil (5-FU), Fig. 1, a well-known anticancer drug, was first synthesized in 1957 [16] and it is being used since then for the treatment of solid tumors [17,18]. It belongs to the family of drugs called antimetabolite. It is a pyrimidine analogue. 5-FU was introduced in the early 1960s as topical chemotherapeutic agent and it has become increasingly accepted because of its efficacy, economy, and relative absence of side effects in treating many pre-cancerous conditions, certain benign and malignant tumors, and dermatoses [19]. However, despite its extensive therapeutic value, there are several side effects with usage of this drug [20]. 5-FU is inactivated by pyrimidine ring reduction carried out by dihydrouracil dehydrogenase, whose high turn over markedly impairs drug efficiency, thus forcing a high dosage and leading to serious cytotoxic effects [21,22].

The vibrational spectra (IR, Raman and FT-Raman) [2,3,13] and SERS [12] of 5-FU have been studied earlier. However, on account of medicinal importance of 5-FU and lack of consensus between the spectral data on it reported in literature, supplementary studies are required on the vibrational spectra of this compound. Therefore, in order to have more consistent interpretation of vibrational spectra, we have reinvestigated the FT-IR and FT-Raman spectra of 5-FU, especially in the solid state, and results are being reported in this paper. In addition the tautomerism in 5-FU was also studied and the spectra of the two most stable forms were simulated.

2. Experimental

5-Fluorouracil (solid state, white crystalline powder, m.p. 300 °C) of spectral grade was obtained from M/s Aldrich chemical (Milwanke, WI, USA) and used as such without any further purification.

* Corresponding author. Tel.: +91 120 2780506.
E-mail addresses: asian_c_l@rediffmail.com, v_krastogi@rediffmail.com (V.K. Rastogi).

1386-1425/$ – see front matter © 2011 Elsevier B.V. All rights reserved.
doi:10.1016/j.saa.2011.04.008

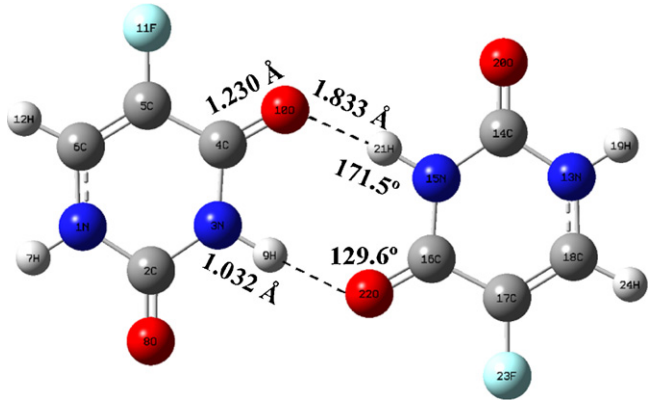

Fig. 1. Optimized dimer form of 5-fluorouracil, with the labelling of the atoms and several parameters of interest.

The mid infrared spectrum of 5-FU from 400–4000 cm^{-1} was recorded with Perkin Elmer FTIR model 1760X instrument using KBr technique with 1 mg sample per 300 mg KBr. For the spectrum acquisition, 4 scans were collected at 4 cm^{-1} resolution, Fig. 2b.

The FT-Raman spectrum of 5-fluorouracil was recorded at room temperature in the powder form in the region 50–4000 cm^{-1} on a Bruker IFS66 optical bench with an FRA 106 Raman module attachment. The sample was mounted on the sample illuminator using an optical mount and no sample pretreatment was undertaken. The NIR output (1064 nm) of an Nd: YAG laser was used to excite (the probe) the spectrum. The instrument was equipped with a liquid-nitrogen-cooled Ge detector. The laser power was set at 100 mW and the spectrum was recorded over 1000 scans at a fixed temperature. The spectral resolution was 6.0 cm^{-1} after apodisation (Fig. 4).

3. Calculations

Quantum chemical calculations using density functional methods (DFT) were performed, mainly with B3LYP, implemented in the GAUSSIAN 03 program package [23]. For the optimization process, 6-31G** and 6-311++(3df,pd) basis set, as well as DGDZVP were utilized. B3LYP was selected for its better accuracy in the wavenumber calculations [9,24]. Full optimization was performed with the option TIGHT and wavenumber calculations were carried out to asses that all the geometries correspond to stationary points (no negative eigenvalue) and as well to predict the theoretical IR and Raman spectra, Table 1 and Figs. 3 and 4.

In solid state 5-FU was simulated in a dimer form, Fig. 1. This dimer was the only one found in the crystal of 5-FU [25], and it is planar and symmetric. The calculated wavenumbers were collected in Table 2, while the simulated IR and Raman spectra with scaled wavenumbers were plotted for comparison purposes in Figs. 3 and 4.

4. Results and discussion

4.1. Isolated state

5-FU is a planar, six membered N-heterocyclic ring molecule, which exhibits 30 normal modes of vibrations, 21 of which are in-plane (a′ species) and 9 are out-of-plane (a″ species). Table 1 shows the reported FT-IR wavenumbers in Ar matrix [13], 10th column. In order to help in the analysis and assignment of the observed wavenumbers, DFT computations of the vibrational spectra were carried out and included in the first two columns of Table 1. The level of earlier [2] calculations was improved in the present paper with the B3LYP/6-311++G(3df,pd) level, the fourth column. We have demonstrated [8,9,24,26], that the computed wavenumbers at the B3P86 and B3LYP/6-31G** DFT methods yield fairly good wavenumbers.

The characterization of the local modes is shown by using the definition of the uracil ring normal modes [26], in 11th column of Table 1. The calculated % potential energy distribution (PED) of the different modes for each vibration appears in the last column of the same table. Contributions lower than 10% were not considered.

An improvement can be carried out in the computed wavenumbers by the use of scaling procedures. To scale the wavenumbers, the simplest procedure is using an overall scale factor, which is the procedure generally applied in the literature [24], but it leads to a high error in the scaled values and impede a clear and accurate assignment of modes. Thus to reduce this error and get a trustworthy assignment two accurate scaling procedures can be

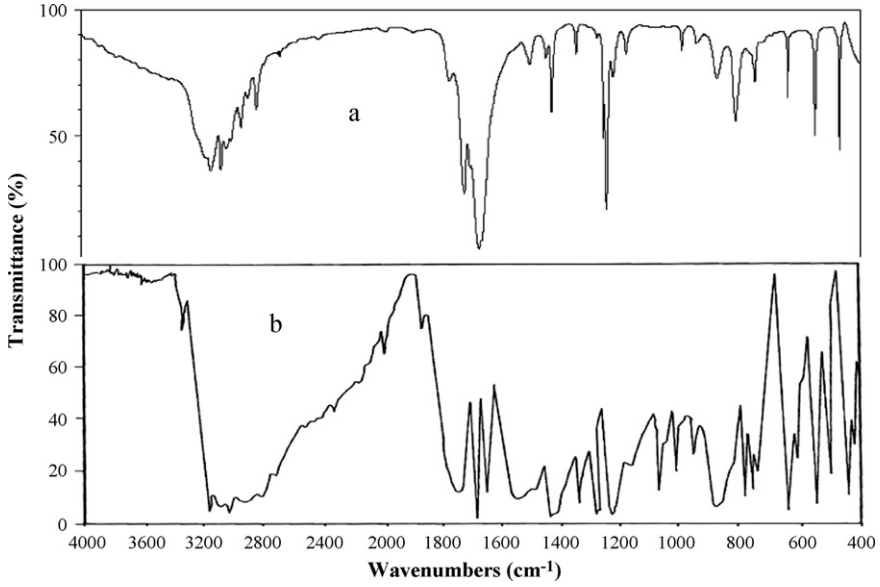

Fig. 2. Experimental IR spectra of 5-flurouracil: (a) from Ref. [42]. (b) Our spectrum at higher concentration of the sample.

Table 1
Vibrational wavenumbers (ω, cm^{-1}) calculated in the isolated state of 5-fluorouracil at HF, B3P86 and B3LYP/6-31G** levels, scaled values and experimental IR data in Ar matrix (ν, cm^{-1}).

Calculated, ω					Scaled[c]				Exp.	No.[d]	Characterization[e]
HF	B3P86	B3LYP	B3LYP[a]	Anh[b]	HF	B3P86	B3LYP	B3LYP[a]	ν [13]		
3904	3686	3662	3644.0	3476	3491	3495	3494	3498.1	3480.0	30	100%, ν(N1–H)
3859	3640	3617	3594.9	3434	3451	3452	3452	3451.4	3427.5	29	100%, ν(N3–H)
3414	3258	3243	3221.1	3134	3054	3093	3098	3095.8		27	100%, ν(C6–H)
2021	1868	1846	1803.1	1776	1810	1788	1779	1747.0	1780.0	26	78%, ν(C2=O) + 11%, ν(C4=O) + 10%, δ(N–H)
2004	1835	1813	1778.5	1733	1795	1757	1747	1723.6	1746.5	25	76%, ν(C4=O) + 11%, ν(C2=O) + 10%, δ(N3–H)
1920	1749	1732	1712.2	1677	1720	1676	1671	1660.5	1686.5	24	70%, ν(C5=C6) + 20%, ν(ring)
1656	1524	1507	1498.3	1448	1484	1465	1458	1457.1	1472.0	23	60%, δ(N1–H) + 38%, ν(ring)
1574	1445	1431	1425.2	1395	1411	1391	1386	1387.6	1400.5	22	65%, ν(ring) + 30%, δ(N1–H)
1551	1401	1398	1404.4	1340	1390	1349	1355	1367.8	1367.0	20	75%, δ(N3–H) + 14%, δ(N1–H) + 10%, δ(ring)
1490	1362	1355	1351.2	1319	1336	1313	1315	1317.2	1333.5	21	65%, δ(C6–H) + 20%, ν(ring) + 13%, δ(N1–H)
1386	1308	1285	1260.7	1225	1243	1262	1249	1231.1	1247.5	28	60%, ν(C–F) + 38%, ν(ring)
1318	1205	1187	1182.7	1144	1182	1165	1156	1156.9	1184.0	18	42%, δ(C6–H) + 36%, δ(N3–H) + 20%, δ(ring)
1245	1171	1160	1156.8	1129	1117	1134	1130	1132.2	1147.0	19	45%, δ(CCH) + 40%, δ(N1–H) + 15%, δ(ring)
1057	978	969	969.5	923	949	952	950	954.1	959.5	14	38%, δ(N3–H) + 35%, δ(C6–H) + 25%, δ(ring)
1028	887	888	906.2	880	923	867	873	893.9	876.5	15	97%, γ(C6–H)
893	822	817	819.5	791	803	806	806	811.4	806.5	17	100%, δ(ring)
855	754	748	772.0	747	769	742	741	766.2	757.5	12	100%, δ(ring)
835	753	746	758.3	697	751	741	739	753.2	749.5	11	53%, γ(C2=O) + 34%, γ(C4=O) + 13%, γ(ring)
799	748	741	741.5	744	719	736	735	737.2		10	68%, γ(C–N3–H) + 32%, γ(ring + C4=O)
722	678	674	667.5	643	650	671	671	666.8	653.0	9	95%, γ(N3–H)
686	630	628	633.8	616	618	626	628	634.8		7	100%, δ(ring)
587	554	545	539.5	528	530	554	549	545.1	527.0	8	98%, γ(N1–H)
559	538	536	538.4	519	505	539	541	544.0	532.0	5	100%, 6b[f], δ(ring)
492	456	455	457.9	470	445	462	464	467.4	451.0	16	43%, δ(C–F) + 32%, δ(C=O) + 25%, δ(ring)
430	389	388	391.2	385	390	399	401	404.0		3	70%, δ(OCNCO) + 30%, δ(ring)
409	378	377	383.5	354	371	389	391	396.7		4	68%, γ(C=C–H) + 32%, γ(ring)
380	352	347	345.0	342	345	365	362	360.1		13	75%, γ(NC=CF) + 25%, γ(ring)
326	299	300	307.4	307	297	315	318	324.3		6	80%, δ(OCCF) + 20%, δ(ring)
168	115	153	153.1	131	156	142	179	177.5		1	47%, γ(C=O) + 35%, γ(N3–H) + 18%, γ(ring)
124	119	117	115.6	129	116	146	145	141.9		2	37%, γ(C=O) + 29%, γ(C–F) + 22%, γ(N1–H) + 12%, γ(ring)

[a] At the B3LYP/6-311++G(3df,pd) level.
[b] Anharmonic calculations at the B3LYP/6-31++G** level, Ref. [27].
[c] With the scaling equations: $\nu_{scaled,\ HF} = 5.7 + 0.8928 \cdot \omega_{calculated,\ HF}$; $\nu_{scaled,\ B3P86} = 34.1 + 0.9389 \cdot \omega_{calculated,\ B3P86}$; $\nu_{scaled,\ B3LYP} = 34.6 + 0.9447 \cdot \omega_{calculated,\ B3LYP}$, from Refs. [9,26]; and $\nu_{scaled,\ B3LYP/6\text{-}311++G(3df,pd)} = 31.9 + 0.9512 \cdot \omega_{calculated,\ B3LYP/6\text{-}311++G(3df,pd)}$, Ref. [1a].
[d] According to the notation of the uracil ring modes, Ref. [26].
[e] With B3P86, Ref. [2].
[f] The direction of the displacement vectors is analogous to mode 6b of benzene ring [24].

employed [9]: the scaling equation and the specific scale factors for each mode. Both procedures require the previous calculated wavenumbers of the uracil molecule [26] determined at the same computational level.

For the scaling equation procedure, the linear regression between the calculated and experimental wavenumbers obtained with the 6-31G** basis set in uracil molecule gives a correlation coefficient of 0.9999, similar to that obtained with the larger 6-311++G(3df,pd) and with analogous standard deviation. For this reason, the results with this basis set were selected for the discussion in the present study. On the other hand, the specific scale factors for each mode procedure leads to the lowest errors, although it requires more effort and with high basis set the difference is insignificant. Thus for simplicity, Table 1 shows only the scaled wavenumbers obtained with this scaling equation procedure, 6–9th columns. These scaled wavenumbers can be directly compared to those observed in the IR spectra in Ar matrix, 10th column. For comparison purposes, the 5th column lists the reported anharmonic data [27]. The error obtained with these anharmonic data is similar to ours scaled values, but our scaling procedure is simpler.

Therefore, the assignments proposed for the experimental wavenumbers, and listed in the last column, are in agreement with earlier determinations in uracil molecule [28,29] and in related ones [2–7]. The assignments for several observed modes in the present study are obvious and require no further discussion, and therefore only a brief analysis is given here for them.

4.2. Solid state

The existence of H-bonding of the type C=O. . .H–N in uracil and its derivatives has been confirmed [2,7]. The intermolecular forces (hydrogen bonding) present in the solid state play a dominant role in modifying the magnitudes and intensities of the wavenumbers appearing in the IR and Raman spectra. Thus, for some of the calculated wavenumbers and Raman scattering activities are observed significant deviations, especially those involved in hydrogen bonds. For this reason, and to improve the accuracy in the assignment of the IR and Raman bands observed in the solid state sample, a dimer form was simulated. The computed results appear collected in Table 2 together with the experimental IR data in KBr pellets and Raman data in the solid state. The scaled harmonic vibrational bands determined in the isolated state and in the dimer form are plotted in Figs. 3 and 4.

The first column of Table 2 lists the calculated wavenumbers in cm^{-1}. Due to the symmetry of the dimer, for each vibration appears two wavenumbers, with very close values in the majority of the cases. Of these two wavenumbers, that one with the highest IR intensity is shown in bold type. In each vibration of the dimer the discussion is mainly centered in the wavenumbers with higher

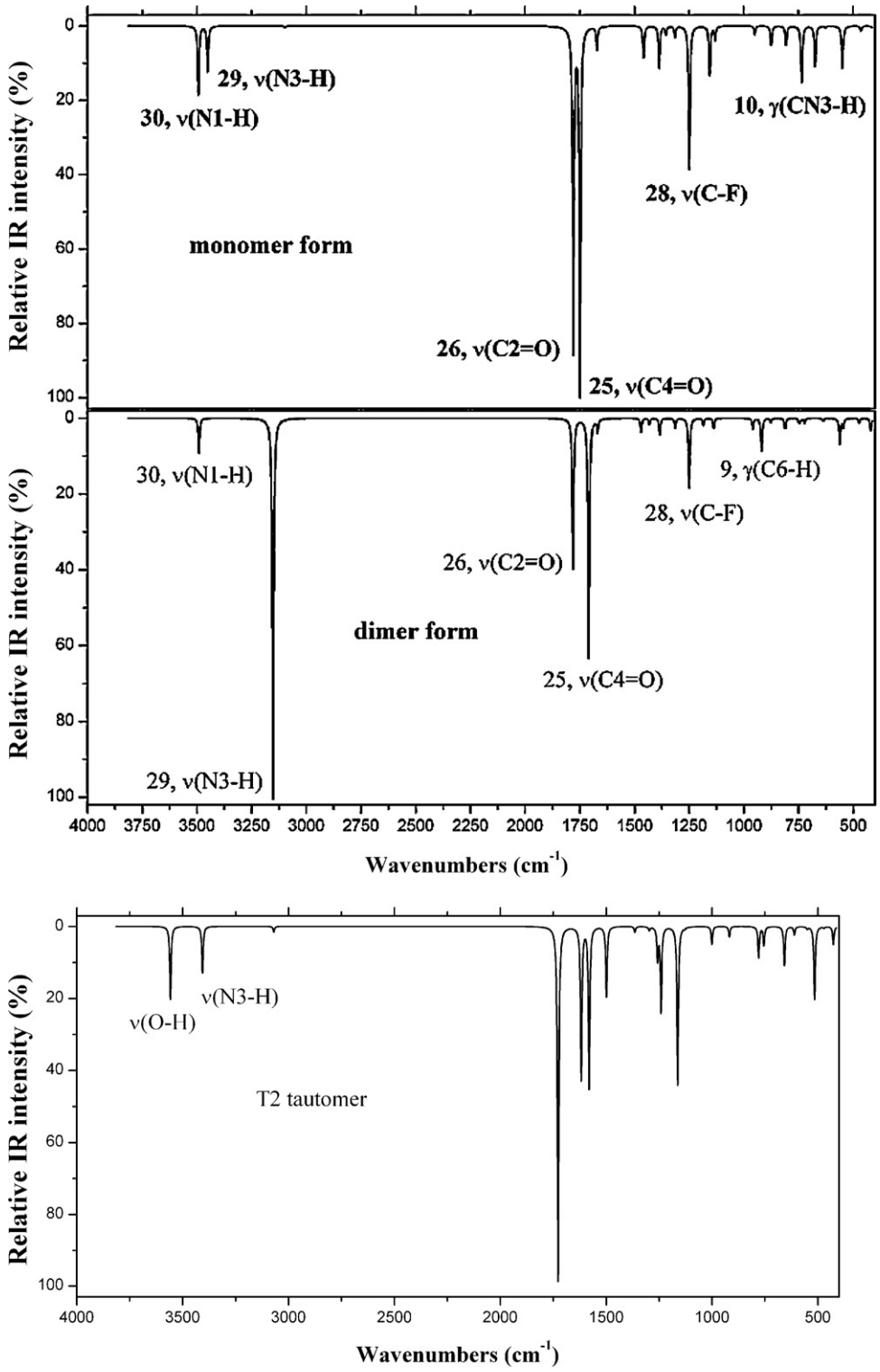

Fig. 3. Simulated scaled IR spectrum at the B3LYP level: in the isolated state (monomer form), in the dimer form, and in the isolated state of tautomer T2.

intensity. The second column collects their relative infrared intensities (A) in %. They were obtained by normalizing the computed value to the intensity of the strongest band, the ν(N3–H) mode. Of the two values for each mode, in bold type appear the higher value and also its corresponding scaled wavenumber, column 4th. The relative Raman intensities (*S*), 3rd column, were also normalized with the intensity of the ν(N3–H) mode. It is noted that the highest IR and Raman intensities appear in different modes of those in the isolated state.

4.3. Assignment of the different vibrations

The discussion is mainly centered in a comparison of the scaled B3LYP/6-31G** results in the isolated state (monomer form) with the dimer results and with the experimental wavenumbers.

4.3.1. N–H/C–H modes

Stretching modes. In the isolated state, the scaled values at 3494 and 3452 cm^{-1}, corresponding to the ν(N1–H) and ν(N3–H) modes,

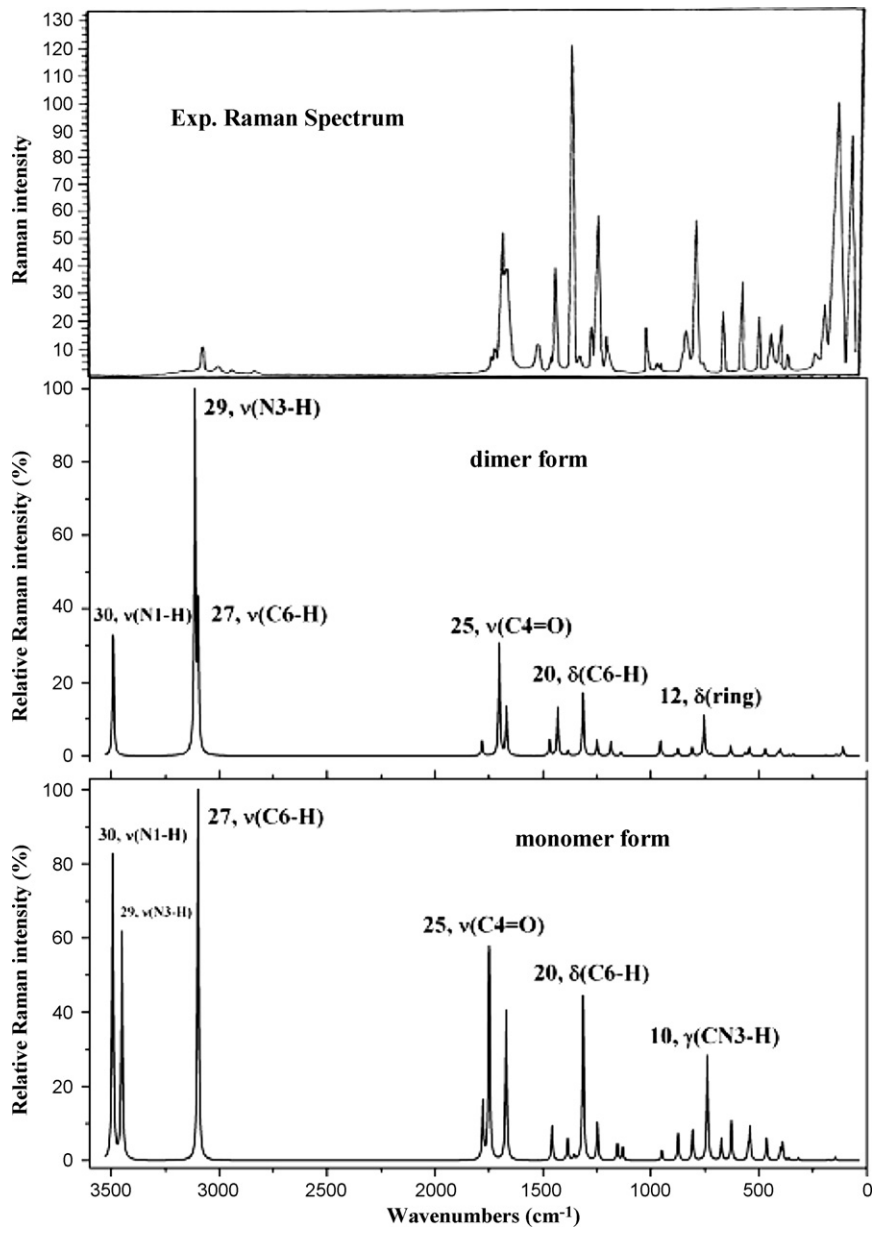

Fig. 4. Comparison of the experimental Raman spectra of 5-FU with the simulated scaled IR spectrum at the B3LYP level: in the isolated state (monomer form), and in the dimer form.

respectively, are in excellent accordance with the experimental IR bands observed in Ar matrix at 3480.0 and 3427.5 cm^{-1}, respectively. The N–H oscillators appear to be uncoupled, and the ν(N1–H) band is estimated [2,13] to occur at wavenumber higher than that of ν(N3–H) band.

In the solid state the N–H stretching region exhibits a broad band, Fig. 2, originated from the hydrogen-bonded network, in which the determination of the fundamental modes is difficult. In our simulation with the dimer form, only N3–H group is involved in H-bonds and ν(N3–H) appears moved ca. 300 cm^{-1} to lower wavenumbers. Moreover, this ν(N3–H) mode appears with the highest IR and Raman intensity on the scaled wavenumbers at 3152 and 3112 cm^{-1}, respectively, Figs. 3 and 4, in agreement with the observed bands at 3067 cm^{-1} (IR) and 3066.5 cm^{-1} (Raman). The small difference (40–90 cm^{-1}) could indicate a stronger H-bond in the crystal. However, this tentative assignment contradicts that reported by other authors.

In the isolated state, the ν(N1–H) stretching is easily identified and the scaled value is correctly assigned to the Ar matrix band. However, in the solid state our simplified model does not consider the N1–H. . .O=C intermolecular H-bond of the crystal [25]. Thus, it is expected a similar displacement of ca. 300 cm^{-1} in this ν(N1–H) mode, as was observed in ν(N3–H), and a remarkable enhancement of its IR and Raman intensities. The scaled wavenumber at 3491 → 3191 cm^{-1} (predicted) appears in agreement with the Raman band at 3142.9 cm^{-1}.

In the experimental IR and Raman spectra bands have not been detected in the 3500–3200 cm^{-1} range, which indicates that the N1–H and N3–H groups appear involved in an intermolecular H-bond net, as it is observed in the crystal [25]. In this net, weak C–H. . .O=C intermolecular H-bonds can be identified, due to which ν(C–H) mode moves to lower wavenumbers, but its IR intensity is always remarkably lower than those of the ν(N–H) modes, and for this reason, we have tentatively changed the assignment of these bands.

In the isolated state the ν(C–H) mode is predicted almost pure and IR inactive in accordance to its no-detection in the Ar matrix spectrum. Dobrowolski et al. [13] have assigned this mode below

Table 2
Comparison of the calculated harmonic vibrational wavenumbers (ω, cm^{-1}) in the dimer form of 5-fluorouracil at the B3LYP/6-31G** level, Relative infrared intensities (*A*, %), relative Raman scattering activities (*S*, %), scaled wavenumbers and experimental IR and Raman data (cm^{-1}) in the solid state of 5-FU.

Calculated			Scaled[a]	Experimental IR		Experimental Raman			No.[c]	Characterization
ω	*A*	*S*		Ref. [27]	ν[b]	SERS, Ref. [12].	ν[b]	Ref. [2]		
3659	9	37	3491	**3141 vs**	3135	3146 sh		3142.9	30	ν(N1–H)
3300, 3258	**100**, 0	0, 100	**3152**, 3112	**3069 vs**	3067	3073 w	3069	3066.5	29	ν(N3–H)
3243	0	28	3098	**3001 vs**	3020	3001 vw		3002.0, 3028.1	27	ν(C6–H)
						2932,2892,2824 vw		2934.2, 2450.2, 2820.9		Combinations modes
1851, **1849**	0, **39**	3, 0	1783, **1781**	**1722 s**	1720	1725 vw, 1707 vw	1706	1724.5, 1704.9	26	ν(C2=O) + ν(C4=O) + δ(N–H)
1773, 1766	**63**, 0	0, 22	**1710**, 1703	**1671 vs**	1670	1672 m	1671	1670.4	25	ν(C4=O) + ν(C2=O) + δ(N3–H)
1731, **1730**	0, **3**	9, 0	1670, **1669**	**1662 vs**	1650	1659 w	1655	1658.3	24	ν(C5=C6) + ν(ring)
1520, 1519	**4**, 0	0, 3	**1471**, 1470	**1502 m**	–	1506 vw	1504	1503.6	23	δ(N1–H) + ν(ring)
1480, 1479	**2**, 0	0, 9	**1433**, 1432	**1430 s**	1435	1447 vw, 1425 w	1425	1448.2, 1424.1	22	ν(ring) + δ(N1–H)
1429	4	1	1385	**1349 m**	1345	1350 vs	1349	1348.5	20	δ(N3–H) + δ(N1–H) + δ(ring)
				1312 w		1313 vw		1311.3, 1119.3		Combinations modes
1355, **1354**	0, **2**	11, 0	1315,**1314**		1260	1258 w	1257	1256.8	21	δ(C6–H) + ν(ring) + δ(N1–H)
1287, 1286	**18**, 0	0, 3	**1250**, 1249	**1225 m**	1222	1225 m	1226	1224.0	28	ν(C–F) + ν(ring)
1219, **1218**	0, **2**	2, 0	1186, **1185**	**1181 m**		1187 vw	1185	1186.8	18	δ(C6–H) + δ(N3–H) + δ(ring)
1169	3	1	1139	**1158 sh**	970	987 vw	996	996.3, 985.5	19	δ(CCH) + δ(N1–H) + δ(ring)
979, 975	**3**, 0	0, 2	**959**, 956	**949 w**		950 vw		949.5	14	δ(N3–H) + δ(C6–H) + δ(ring)
937, 908	**9**, 0	0, 0	**920**, 892			937 vw		936.0	9	γ(N3–H)
892, 890	**1**, 0	0, 1	**877**, 875	**880 m**	875	887 vw		894.8	15	γ(C6–H)
823, 820	**3**, 0	0, 1	**812**, 809	**813 s**		810 vw	811	809.1	17	δ(ring)
762, **755**	0, **1**	6, 0	754, **748**	**771 w**		779 sh, 769 m	768	767.9	12	δ(ring)
748, 747	**1**, 0	0, 0	**741**, 740	**751 m**	740	738 vw		734.7	11	γ(C2=O) + γ(C4=O) + γ(ring)
728	1	0	722	**730 w**					10	γ(C–N3–H) + γ(ring)
639, 631	**1**, 0	0, 2	**638**, 631	**643 m, 635 vw**	615	639 w, 634 vw	637	638.3, 633.5	7	δ(ring)
559, 558	**7**, 0	0, 0	**563**, 562						8	γ(N1–H)
541, 539	**2**, 0	0, 1	**546**, 544	**551 s, 517 w**	546	546 w	546	545.2	5	6b[d], δ(ring)
464, 462	**1**, 0	0, 1	**473**, 471	**469 s**	450	466 sh, 471 w	470	470.0, 464	16	δ(C–F) + δ(C=O) + δ(ring)
408, 398	**3**, 0	0, 0	**420**, 411	**419**	419	414 vw	413	414	3	δ(OCNCO) + δ(ring)
388, **383**	0, **1**	1, 0	401, **396**			399 sh, 366 vw	367	365	4	γ(C=C–H) + γ(ring)
346	1	0	361			372 vw		371	13	γ(NC=CF) + γ(ring)
324, **321**	0, **0.2**	0, 0	341, **338**			333 vw	332	331	6	δ(OCCF) + δ(ring)
177, 165	0	0, 0	202, 190			207 vw	210	207	1	γ(C=O) + γ(N3–H) + γ(ring)
117, 116	**0.2**, 0	0, 0	**145**, 144			167 vw	166	167	2	γ(C=O) + γ(C–F) + γ(N1–H) + γ(ring)
111,80	0	0, 1	139, 110			110 ms	110	109		Lattice modes
77,**65**	0, **0.2**	0, 0	107, **96**			92, 83, 68		91, 81, 76, 56		Lattice modes

[a] With the scaling equation: $\nu_{scaled} = 34.6 + 0.9447 \cdot \omega_{calculated}$, Refs. [9,26].
[b] Present work.
[c] According to the notation of the uracil ring modes, Ref. [26].
[d] The direction of the displacement vectors is analogous to mode 6b of benzene ring [24].

ν(N3–H) mode in 5-halouracils. In the solid state this mode also appears IR inactive and with medium Raman activity. It is noted (Fig. 4), that in the isolated state (monomer form), ν(C6–H) mode appears with the highest Raman intensity, while in the dimer form this intensity is remarkably reduced, being ν(N3–H) the mode that appears with the highest Raman intensity. This fact could originate the mistake in its assignment. Thus, on the basis of computed Raman intensity, we have tentatively assigned the observed [2] Raman wavenumber 3002.0 cm^{-1} to the ν(C6–H) mode. This criterion is in contrast to that reported by Paval et al. [12], assigning the peak at 3073 cm^{-1} (B3LYP/6-311 + G*; calculated: 3104 cm^{-1}) to this mode. Our simulation with the dimer form, clarify something the assignment, but a more complex simulation of the solid state could be appreciated.

In-plane bending modes. In general, all the vibrations in the 1760–950 cm^{-1} range have significant contributions of δ(N–H) modes. The main contributions correspond to mode no. 23 (ring normal mode no. 23 in uracil [26]) δ(N1–H), and no. 20, δ(N3–H), scaled in the isolated state at 1458 and 1355 cm^{-1}, respectively, and strongly coupled with ν(C–N) modes. These wavenumbers are in accordance with the experimental IR values in Ar matrix at 1472.0 and 1367.0 cm^{-1}, respectively, and with the literature data.

In the solid state δ(N3–H) mode (no. 20) is involved in strong H-bonds. Thus, it is scaled at 1433 cm^{-1}, and it is related to the Raman band at 1424.1 cm^{-1}, indicating a blue-shift in this mode of 58 cm^{-1}. Mode no. 14 appears at similar wavenumber that in the isolated state, and it was related to the weak Raman band at 949.5 cm^{-1}.

δ(C6–H) mode (nos. 21, 18) is strongly coupled with C=C, C–N and N–H bending modes, and it was related to the Raman bands at 1256.8 and 1186.8 cm^{-1}, respectively.

Out-of-plane bending modes. In the isolated state the γ(N3–H) mode (no. 9) is scaled at 671 cm^{-1} in good accordance to the IR band in Ar matrix at 653.0 cm^{-1}. Analogously, γ(N1–H) mode (no. 8), scaled at 549 cm^{-1} is related to the Ar matrix band at 527.0 cm^{-1}. These modes appear almost pure, with 95-98% PED.

In the solid state, mode γ(N3–H) appears moved by 220–250 cm^{-1} to higher wavenumber in accordance to the red-shift observed in its stretching band. The weak Raman band at 936.0 cm^{-1} was assigned to this mode, in contrast to that reported by other authors [12,27]. Mode γ(N1–H) is also expected to move to higher wavenumber, 563 cm^{-1} (scaled) → 780 cm^{-1} (predicted).

Mode γ(C6–H), an almost pure mode (97% PED), appears scaled at 873 cm^{-1} in accordance with the Ar matrix band at 876.5 cm^{-1}. In the solid state this mode is expected to appear also at a slightly higher wavenumber, in accordance to the small red-shift of its stretching mode. Thus, the Raman band detected at 894.8 cm^{-1} was assigned to this mode.

4.3.2. C=O/C=C stretching modes

In the experimental spectra of uracil and 5-halouracils, one can expect two bands due to C=O stretching modes. The fluorine atom has a significant influence on the positions of ν(C=O) modes. The halogen effect on C4=O group is stronger than on C2=O group, which is located far to the fluorine atom, and moreover, it is surrounded by the two N–H groups, which buffer it from influence of the remaining molecular moieties [13].

In the isolated state ν(C2=O) and ν(C4=O) stretchings appear slightly coupled with δ(N–H) modes and scaled at 1779 and 1747 cm^{-1}, respectively, in excellent accordance to the Ar matrix data at 1780.0 and 1746.5 cm^{-1}. In the solid state and due to the H-bonds, their wavenumbers appear at slightly lower values. As both oxygen atoms are involved in H-bonds, both ν(C2=O) and ν(C4=O) modes decrease in wavenumber. Thus, the two lines observed in the IR and Raman spectra of the solid state at 1724.5/1704.9 and 1670.4 cm^{-1}, can be clearly assigned to C2=O and C4=O stretching vibrations. Pavel et al. [12] have assigned these modes at 1725 and 1672 cm^{-1}, respectively. These assignments find further support from literature values [3,8,9,11,12].

ν(C=C) mode, scaled at 1671 cm^{-1} can be easily related to the band at 1686.5 cm^{-1} by Dobrowolski et al. [13] in the Ar-matrix IR spectra. In the solid state the bands appearing at 1650 cm^{-1} in IR and at 1658.3 cm^{-1} in Raman are assigned to this mode. This assignment agrees very well with the literature value [12]. The small 30 cm^{-1} red-shift observed experimentally is due to the effects of the H-bonds on H6 and in general on the ring structure. This mode was found to be sensitive to the nature of the X-substituents [8,13,30,31].

4.3.3. Ring modes

In general, all the vibrations appeared under 1500 cm^{-1} have significant contributions of ring modes. The main contributions correspond to modes nos. 22 and 18 (stretching), to nos. 17, 12, 7 and 5 (in-plane bendings), and to 13 and 10 (out-of-plane bending). The description of mode 22 is complex, mainly because it appears strongly coupled to δ(N1–H) mode. In general, the other ring stretching modes are in conformity with the literature values [9–13].

4.3.4. C–F modes

ν(C–F) stretching mode usually appears in the 1000–1450 cm^{-1} region and with strong intensity, in both the Raman and infrared spectra. On the basis of theoretical spectra at B3PW91/6-311G** level Dobrowolski et al. [13] have identified this mode in Ar matrix at 1247.5 cm^{-1}, in accordance to our scaled value at 1249 cm^{-1}. For fluorothymines the C–F stretching mode was assigned at ~1160 cm^{-1} by Stepanian et al. [32]. The C–F moiety is expected to be affected little by the H-bonds. Thus, in the solid state the medium intense band appearing in Raman at 1224.0 cm^{-1} and at 1222 cm^{-1} in IR could be assigned to this C–F stretching mode. This assignment is further supported by the literature data [33].

In the study on 5-halouracils, Dobrowolski et al. [13] place the in-plane δ(C–F) mode below the out-of-plane γ(C–F) mode. However, our earlier [2] theoretical computation at the ab initio and DFT levels place the in-plane δ(C–F) mode (~450 cm^{-1}) above the out-of-plane γ(C–F) mode (~350 cm^{-1}) [2]. Therefore, in the present study the observed wavenumbers at 464 and 331 cm^{-1} in Raman spectrum are assigned to in-plane and out-of-plane C–F modes, respectively. This assignment is further supported by literature values [12,33,34].

4.4. Tautomerism

It is well known that most carbonyl compounds exist almost exclusively in their *keto* form at equilibrium and it is usually difficult to isolate the pure *enol* form. The molecular modeling of a single structure does not include any intermolecular interactions and thus it is equivalent to predicting the monomeric structure in the vapor phase [12]. Theoretical studies have shown that *keto-enol* tautomerism exists in nucleic acid base derivatives [35,36]. Therefore it has been reported that, the hydration favored the tautomerism, and in 5-bromouracil (5-BrU) the *enol* tautomer T2 is more stable than the *keto* one [37]. Previously, we have studied the tautomerism in 5-IU [38], and in 5-BrU [39]. Now, in the present paper is briefly analyzed the tautomerism of 5-FU. The importance of this tautomerism has been indicated by Pavel et al. [12].

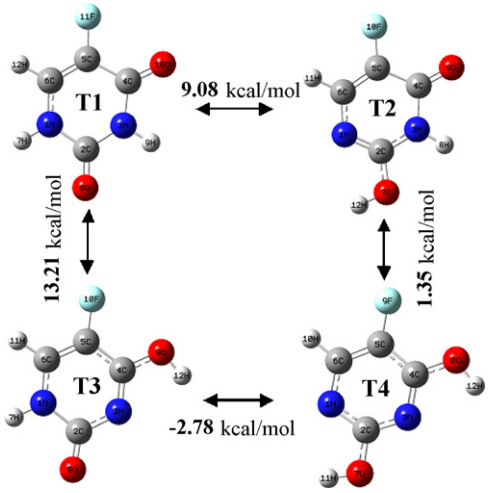

Fig. 5. Tautomerism in 5-fluorouracil. The energies were calculated at MP2/6-31G** level. Tautomer T3 is the least stable of the four tautomers plotted.

Fig. 5 shows the four most stable tautomers, together with their differences in energy calculated at the MP2/6-31G** level. These values appear somewhat lower than those found in uracil, but they are similar to those computed in 5-BrU. Tautomer T2 is the most stable *enol* form. The stability order is T1 > T2 > T4 > T3. The other possible tautomers, not included in Fig. 5, are remarkably less stable and thus they were not plotted.

Although in the isolated state 5-FU may exhibit tautomerism, however, the absence of ν(OH) band in the region 3500–3700 cm^{-1} (Figs. 3 and 4) and appearance of ν(C=O) modes in the region 1600–1750 cm^{-1} as strong bands in the spectra indicates that in the solid state 5-FU exists only in *keto* form.

Table 3
Theoretical computed heat of formation, zero-point vibrational energies, rotational constants, entropies and dipole moments in 5-FU and uracil molecules at the B3LYP/6-31G** level.

Parameters	Uracil monomer	5-FU monomer	5-FU dimer
Total energy + ZPE (AU)	−414.738606	−513.965229	−1027.951529
Gibbs Free energy (AU)	−414.769030	−513.996983	−1027.997575
Rotational constants (GHz)	3.87	3.19	0.70
	2.00	1.40	0.21
	1.32	0.97	0.16
Entropy (cal mol^{-1} K^{-1})			
Total	79.0	83.7	132.2
Translational	40.1	40.5	42.6
Rotational	27.8	28.7	33.8
Vibrational	11.1	14.5	55.7
Dipole moments (Debyes)	4.248	3.888	0.010

4.5. Thermodynamical functions

Calculated wavenumbers have been employed to yield thermodynamic properties, which are collected in Table 3. The theoretical data are employed to correct experimental thermochemical information at 0 K, as well as for the effect of the zero-point vibrational energy (ZPVE). For the ZPEV, scaling factors can be used [40] to improve their overestimation.

The entropies calculated for several kinds of compounds and at different ab initio levels have been reported [41] to have mean absolute deviations less than 5%, as compared to the experimental data. The differences have been attributed to the neglect of residual (orientation) entropy present at 0 K in the crystal. With the dimer formation, a notorious reduction in the entropy is observed.

5. Summary and conclusions

The most important findings of the present work are the following:

(1) Overall the assignment to various bands observed in IR and Raman spectra find support from calculations and are consistent with the previous findings. The deviation between the theoretical and experimental results in some cases may be due partly to the anharmonicity and partly to the fact that most quantum chemical methods overestimate force constants at the exact equilibrium geometry.
(2) The simulation of 5-FU in the solid state as the dimer form produces a remarkable change in the wavenumbers and intensities of the modes involved in H-bonds.
(3) N3–H and N1–H are the groups that are mainly involved in C═O. . .N–H bonds and hence the lowering in wavenumber of their stretching modes, increasing in the out-of-plane modes, and a remarkable enhancement of their stretching IR and Raman intensities. Thus, the present assignment alters some of our earlier assignments in the solid state. e.g. the assignment to ν(C6–H) mode is done at lower wavenumber than ν(N3–H) mode.

Acknowledgements

MAP is grateful to the UCM of Spain for financial supports through UCM-BSCH GR35/10-A grant number 921628, and to the MCI through CTQ2010-18564 (subprogram BQU). VKR is grateful to Professor N.K. Taneja, Vice-Chancellor, and Prof Ashok Kumar, Head Physics Department, C.C.S. University, Meerut India for providing necessary facilities and to Dr. Shewta Garg (MD) and Dr. Sandip Garg (MD) for useful discussion during the course of this work. VKR is also grateful to DST, New Delhi, India for the award of Project B-65.

References

[1] (a) M. Alcolea Palafox, J. Talaya, A. Guerrero-Martínez, G. Tardajos, H. Kumar, J.K. Vats, V.K. Rastogi, Spectrosc. Lett. 43 (2010) 51–59;
(b) T. Bourova, G. Ten, S. Andreeva, V. Berezin, J. Raman Spectrosc. 31 (2000) 827–836;
(c) M. Alcolea Palafox, V.K. Rastogi, A. Guerrero-Martínez, G. Tardajos, H. Joe, J.K. Vats, Vib. Spectrosc. 52 (2010) 108–121;
(d) M. Alcolea Palafox, G. Tardajos, A. Guerrero-Martínez, V.K. Rastogi, D. Mishra, S.P. Ojha, W. Kiefer, Chem. Phys. 340 (2007) 17–31.
[2] V.K. Rastogi, V. Jain, R.A. Yadav, C. Singh, M. Alcolea Palafox, J. Raman Spectrosc. 31 (2000) 595–603.
[3] V.K. Rastogi, H.P. Mital, S.N. Sharma, in: R.J.S. Clark, D.A. Long (Eds.), Proceedings of XIth International Conference on Raman spectroscopy, John Wiley & Sons, Chichester, 1988, p. 87.
[4] L. Harsány, P. Császár, A. Császár, J.E. Boggs, Int. J. Quantum Chem. 29 (1986) 799–815.
[5] A.J. Barnes, M.A. Stuckey, L. Le Gall, Spectrochim. Acta, Part A 40 (1984) 419–431.
[6] M.J. Wojcik, J. Mol. Struct. 219 (1990) 305–310.
[7] V.K. Rastogi, M. Alcolea Palafox, L. Mittal, N. Peica, W. Kiefer, K. Lang, S.P. Ojha, J. Raman Spectrosc. 38 (2007) 1227–1241.
[8] (a) M. Alcolea Palafox, G. Tardajos, A. Guerrero-Martínez, J.K. Vats, H. Joe, V.K. Rastogi, Spectrochim. Acta, Part A 75 (2010) 1261–1269;
(b) M. Alcolea Palafox, O.F. Nielsen, K. Lang, P. Garg, V.K. Rastogi, Asian Chem. Lett. 8 (2004) 81–93;
(c) V.K. Rastogi, C. Singh, V. Jain, M. Alcolea Palafox, J. Raman Spectrosc. 31 (2000) 1005–1012.
[9] M. Alcolea Palafox, V.K. Rastogi, Spectrochim. Acta, Part A 58 (2002) 411–440.
[10] M. Alcolea Palafox, V.K. Rastogi, R.P. Tanwar, L. Mittal, Spectrochim. Acta, Part A 59 (2003) 2473–2486.
[11] V.K. Rastogi, H.P. Mital, S.N. Sharma, Indian J. Phys. 64B (1990) 312.
[12] I. Pavel, S. Cota, S. Cinta-Pinzaru, W. Kiefer, J. Phys. Chem. A 109 (2005) 9945–9952.
[13] J.Cz. Dobrowolski, J.E. Rode, R. Kolos, M.H. Jamróz, K. Bajdor, A.P. Mazurek, J. Phys. Chem. A 109 (2005) 2167–2182.
[14] U. Norinder, J. Mol. Struct. (Theochem.) 151 (1987) 259–269.
[15] S.M. Morris, Mutat. Res. 297 (1993) 39–51.
[16] C. Heidelberger, N.K. Chaudhuri, P. Danneberg, D. Mooren, L. Griesback, Nature 179 (1957) 663–666.
[17] British Nation Formulary, British Medical Association and Royal Pharmaceutical, Society of Great Britain, London, UK, 2003.
[18] J.L. Grem, Invest. New Drugs 18 (2000) 299–313.
[19] PMID: 4046704 (Pubmed-Infrared for MEDLINE).
[20] D.M. Pritchard, A. Jackman, C.S. Potten, J.A. Hickman, Toxicol. Lett. 102 (1998) 19–27.
[21] A.B.P. van Kuilenburg, Eur. J. Cancer 40 (2004) 939–950.
[22] W. Hui, S. Yang, Z. Jun, Syn. React. Inorg. Met.-Org. Nano-Met. Chem. 36 (2006) 313–315.
[23] M.J. Frisch, G.W. Trucks, H.B. Schlegel, G.E. Scuseria, M.A. Robb, J.R. Cheeseman, J.A. Montgomery Jr., T. Vreven, K.N. Kudin, J.C. Burant, J.M. Millam, S.S. Iyengar, J. Tomasi, V. Barone, B. Mennucci, M. Cossi, G. Scalmani, N. Rega, G.A. Petersson, H. Nakatsuji, M. Hada, M. Ehara, K. Toyota, R. Fukuda, J. Hasegawa, M. Ishida, T. Nakajima, Y. Honda, O. Kitao, H. Nakai, M. Klene, X. Li, J.E. Knox, H.P. Hratchian, J.B. Cross, C. Adamo, J. Jaramillo, R. Gomperts, R.E. Stratmann, O. Yazyev, A.J. Austin, R. Cammi, C. Pomelli, J.W. Ochterski, P.Y. Ayala, K. Morokuma, G.A. Voth, P. Salvador, J.J. Dannenberg, V.G. Zakrzewski, S. Dapprich, A.D. Daniels, M.C. Strain, O. Farkas, D.K. Malick, A.D. Rabuck, K. Raghavachari, J.B. Foresman, J.V. Ortiz, Q. Cui, A.G. Baboul, S. Clifford, J. Cioslowski, B.B. Stefanov, G. Liu, A. Liashenko, P. Piskorz, I. Komaromi, R.L. Martin, D.J. Fox, T. Keith, M.A. Al-Laham, C.Y. Peng, A. Nanayakkara, M. Challacombe, P.M.W. Gill, B. Johnson, W. Chen, M.W. Wong, C. Gonzalez, J.A. Pople, Gaussian 03, Revision B.04, Gaussian, Inc., Pittsburgh PA, 2003.
[24] (a) M. Alcolea Palafox, Recent Phys. Dev. Phys. Chem. 2 (1998) 213–232;
(b) M.A. Palafox, Int. J. Quantum Chem. 77 (2000) 661–684.
[25] L. Fallon III, Acta Crystallogr. B29 (1973) 2549–2556.
[26] M. Alcolea Palafox, N. Iza, M. Gil, J. Mol. Struct. (Theochem.) 585 (2002) 69–92.
[27] E. Akalin, S. Akyuz, T. Akyuz, J. Mol. Struct. 834–836 (2007) 477–481.
[28] B. Blicharska, T. Kupka, J. Mol. Struct. 613 (2002) 153–166.
[29] (a) J. Florian, V. Hrouda, Spectrochim. Acta, Part A 49 (1993) 921–938;
(b) M. Graindourze, T. Grootaers, J. Smets, Th. Zeegers-Huyskens, G. Maes, J. Mol. Struct. 237 (1990) 389–410.
[30] Z. Zwierzchowska, K. Dobrosz-Teperek, W. Lewandowski, R. Kolos, K. Bajdor, J.Cz. Dobrowolski, A.P. Mazurek, J. Mol. Struct. 410 (1997) 415–420.
[31] K. Dobrosz-Teperek, Z. Zwierzchowska, W. Lewandowski, K. Bajdor, J.Cz. Dobrowolski, A.P. Mazurek, J. Mol. Struct. 471 (1998) 115–125.
[32] S.G. Stepanian, N.A. Smorygo, G.G. Sheina, E.D. Radchenko, V.D. Vakovleva, T.N. Rusavskaya, E.P. Studentsov, B.A. Ivin, Yu.P. Blagoi, Spectrochim. Acta, Part A 46 (1990) 355–361.
[33] E. Bednarek, J.Cz. Dobrowolski, K. Dobro-Teperek, J. Sitkowski, L. Kozerski, W. Lewandowski, A.P. Mazurek, J. Mol. Struct. 554 (2000) 233–243.
[34] (a) M. Alcolea Palafox, V.K. Rastogi, C. Singh, R.P. Tanwar, Spectrochim. Acta, Part A 57 (2001) 2373–2389;
(b) V.K. Rastogi, M. Alcolea Palafox, R.P. Tanwar, L. Mittal, Spectrochim. Acta, Part. A 58 (2002) 1987–2004.
[35] H. Yekeler, D. Özbakir, J. Mol. Model. 7 (2001) 103–111.
[36] (a) M. Hanus, M. Kabelác, D. Nachtigallová, P. Hobza, Biochemistry 44 (2005) 1701–1707;
(b) S. Millefiori, A. Alparone, Chem. Phys. 303 (2004) 27–36.
[37] V.I. Danilov, T. van Mourik, N. Kurita, H. Wakabayashi, T. Tsukamoto, D.M. Hovorun, J. Phys. Chem. A 113 (2009) 2233–2235.
[38] V.K. Rastogi, M. Alcolea Palafox, A. Guerrero-Martínez, G. Tardajos, J.K. Vats, I. Kostova, S. Schlucker, W. Kiefer, J. Mol. Struct. (Theochem.) 940 (2010) 29–44.
[39] M. Alcolea Palafox, V.K. Rastogi, Hitesh Kumar, I. Kostova, J.K. Vats, Spectrosc. Lett. 44 (2011) 300–306.
[40] (a) H.B. Schlegel, J. Phys. Chem. 88 (1984) 6254–6258;
(b) A.P. Scott, L. Radom, J. Phys. Chem. 100 (1996) 16502–16513.
[41] (a) G. Leroy, M. Sana, C. Wilante, D.R. Temsamani, J. Mol. Struct. (Theochem.) 259 (1992) 369–381;
(b) M. Sana, G. Leroy, Theor. Chim. Acta 77 (1990) 383–394.
[42] http://riob01.ibase.aist.go.jp.